Neurobiology of Disease 124 (2019) 248–262

Contents lists available at ScienceDirect

Neurobiology of Disease

journal homepage: www.elsevier.com/locate/ynbdi

# Pα-syn* mitotoxicity is linked to MAPK activation and involves tau phosphorylation and aggregation at the mitochondria

Diego Grassi[a,b], Natalia Diaz-Perez[c], Laura A. Volpicelli-Daley[d], Corinne Ida Lasmézas[a,b,*]

[a] Department of Immunology and Microbiology, The Scripps Research Institute, Scripps Florida, Jupiter, FL 33458, United States
[b] Department of Neuroscience, The Scripps Research Institute, Scripps Florida, Jupiter, FL 33458, United States
[c] Palm Beach Gardens, FL 33418, United States
[d] Center for Neurodegeneration and Experimental Therapeutics, University of Alabama at Birmingham, Birmingham, AL 35294, United States

ARTICLE INFO

*Keywords:*
Alpha-synuclein
Tau
Parkinson's disease
Primary neurons
Kinases
Neurotoxicity
Mitochondria
Mitophagy

ABSTRACT

We recently identified a truncated and phosphorylated form of α-synuclein, pα-syn*, as a key neurotoxic α-synuclein species found in cultured neurons, as well as in mouse and Parkinson's disease patients' brains. Small pα-syn* aggregates localize to mitochondria and induce mitochondrial damage and fragmentation. Herein, we investigated the molecular basis of pα-syn*-induced toxicity. By immunofluorescence, we found phosphorylated MKK4, JNK, ERK5 and p38 MAPKs in pα-syn* inclusions. pJNK colocalized with pα-syn* at mitochondria and mitochondria-associated ER membranes where it was associated with BiP and pACC1, markers for the ER and energy deprivation, respectively. We also found that pα-syn* aggregates are tightly associated with small ptau aggregates of similar size. Pα-syn*/ptau inclusions localized to areas of mitochondrial damage and to mitophagic vesicles, showing their role in mitochondrial toxicity, mitophagy induction and their removal along with damaged mitochondrial fragments. Several MAPKs may act cooperatively to phosphorylate tau, notably JNK, p38 and GSK3β, a non-MAPK that was also found phosphorylated in the vicinity of pα-syn*/ptau aggregates. These results add insight into the mechanisms by which pα-syn* exerts its toxic effects that include the phosphorylation of several kinases of the MAPK pathway, as well as the formation of ptau at the mitochondrial membrane, likely contributing to mitotoxicity. Thus pα-syn* appears to be the trigger of a series of kinase mediated pathogenic events and a link between α-syn pathology and tau, another protein known to aggregate in Parkinson's disease and other synucleinopathies.

## 1. Introduction

Parkinson's disease (PD) is the second most common age-related neurodegenerative disease after Alzheimer's disease (AD). Approximately 1–2% of the population over the age of 60 suffers from PD (Lang and Lozano, 1998a; Lang and Lozano, 1998b). Motor impairment is due to the degeneration of dopaminergic neurons of the substantia nigra pars compacta (SNpc) and subsequent loss of dopamine innervation in the striatum (Olanow and Tatton, 1999). There is currently no disease-modifying treatment for PD (Fox et al., 2018).

Approximately 85–90% of PD cases are considered idiopathic and constitute the late-onset, common form of PD. Genome-wide association studies have identified 41 genes associated with disease risk (Chang et al., 2017). Mutations in several genes have been shown to increase the risk of PD or cause early-onset PD (*SNCA, GBA, LRRK2, Parkin, PINK1 and DJ-1)* (Dawson and Dawson, 2003; Farrer, 2006; Klein and Schlossmacher, 2007; Martin et al., 2011; Pankratz et al., 2009; Zhao et al., 2016). Alpha-synuclein (α-syn), a 140 amino-acid long protein encoded by *SNCA*, has emerged as a central player in PD including in familial forms linked to mutations and overexpression of α-syn (Athanassiadou et al., 1999; Eriksen et al., 2005; Ki et al., 2007; Kruger et al., 1998; Markopoulou et al., 1999; Spira et al., 2001; Zarranz et al., 2004). In PD patients brains, α-syn undergoes phosphorylation and misfolding, and forms fibrillar aggregates called Lewy bodies (LBs) and Lewy neurites (Spillantini et al., 1997). Alpha-synuclein also accumulates in other disorders such as Dementia with Lewy Bodies (DLB) or multiple systems atrophy, collectively referred to as synucleinopathies (Arima et al., 1998; Forman et al., 2005; Galvin et al., 2001; Lippa et al., 1999; Spillantini et al., 1998). Oligomeric α-syn inhibits long-term potentiation (La Vitola et al., 2018), promotes complex-I dependent mitochondrial dysfunction (Luth et al., 2014) and interacts with Tom 20, a mitochondrial outer membrane protein,

* Corresponding author at: Scripps Florida, 130 Scripps Way 2B2, Jupiter, FL 33458, United States.
*E-mail address:* lasmezas@scripps.edu (C.I. Lasmézas).

https://doi.org/10.1016/j.nbd.2018.11.015
Received 10 October 2018; Accepted 19 November 2018
Available online 22 November 2018
0969-9961/ 

inhibiting mitochondrial protein transport (Di Maio et al., 2016). Mitochondrial dysfunction has emerged as the link between toxin models of PD and α-syn proteinopathy (Betarbet et al., 2006; Yun et al., 2018) and a possible target for therapeutic intervention (Schapira et al., 2014).

We recently identified a non fibrillar neurotoxic form of α-syn that we called pα-syn* (Grassi et al., 2018). Pα-syn* was first identified in cultured neurons seeded with preformed α-syn fibrils (PFFs) that propagate in cultured neurons in a prion-like manner (Hansen et al., 2011; Kordower et al., 2008; Li et al., 2008; Luk et al., 2012; Luk et al., 2009). Pα-syn* is also present in mouse brains injected with PFFs as well as in the brains of PD patients alongside LBs (Grassi et al., 2018). Pα-syn* was found in an N- and C-terminally truncated form and results from the incomplete proteolytic processing of pα-syn fibrils (pα-synF) during their autophagic degradation. Pα-syn* forms small aggregates/inclusions that attach to mitochondrial tubules, induce ER stress and recruit mitochondria-associated ER membranes (MAMs). Pα-syn* also induces inner membrane depolarization, cytochrome C release and metabolic stress as reported by the accumulation of pACC1 tightly associated with pα-syn* aggregates. As a result of pα-syn* induced damage, mitochondria undergo fragmentation and mitophagy. Pα-syn* therefore appears as a major player in α-syn-induced neurotoxicity. The focus of the present study was to gain understanding of the molecular pathways by which pα-syn* exerts mitotoxicity.

Mitogen-activated protein kinases (MAPKs) are activated by diverse extracellular and intracellular stimuli including peptide growth factors, cytokines, hormones, and various cellular stressors such as oxidative stress and endoplasmic reticulum stress. Persistent activation of the MAPK pathway has been implicated in the development of several human diseases including Alzheimer's disease (AD), Parkinson's disease (PD), and amyotrophic lateral sclerosis (ALS)(Kim and Choi, 2010). c-Jun N-terminal kinase (JNK) and p38 MAPKs activation induces the intrinsic apoptotic (mitochondrial) death pathway (Liu and Zhou, 2017) and both kinases are found to be activated in the brains of PD patients (Ferrer et al., 2001; Hunot et al., 2004). Activated p38 phosphorylates parkin, thereby preventing protective parkin-mediated mitophagy in mice overexpressing A53T α-syn (Chen et al., 2018). Another MAPK, extra cellular signal-regulated kinase 5 (ERK5), accumulates in pα-syn aggregates bearing neurons (Volpicelli-Daley et al., 2014a). Collectively, these data point to a role of MAPKs in neurodegenerative mechanisms underlying PD pathogenesis and in particular mitochondrial dysfunction. We therefore decided to investigate the involvement of MAPKs in pα-syn*-induced neurotoxicity.

Tau, a protein well-known to aggregate and form neurofibrillary tangles in Alzheimer's disease, has been shown to aggregate in Parkinson's disease and other synucleinopathies (Haggerty et al., 2011; Irwin et al., 2013; Sengupta et al., 2015). Because small tau aggregates have been shown to localize to mitochondria (Lasagna-Reeves et al., 2011), we investigated if pα-syn* might be a link between pα-syn pathology and the formation of mitochondrial ptau aggregates.

Herein, we show that pα-syn* triggers the activation of several MAPKs including MKK4, JNK, pERK5 and p38 as well as the phosphorylation of tau at the mitochondrial membrane. pTau aggregates are tightly associated with pα-syn*, and both likely act in concert to induce mitochondrial toxicity.

## 2. Material and methods

### 2.1. Antibody list

#### 2.1.1. Primary antibodies

Alpha-syn antibodies specific for phospho-S129 α-syn recognizing pα-synF, but not pα-syn*, were mouse anti pS129 α-syn clone 81A from Biolegend (IF concentration 1/5000, IHC concentration 1/500) and rabbit anti pS129 α-syn antibody GTX54991 from GeneTex (IF concentration 1/350). The alpha-syn antibody specific for pS129 α-syn recognizing pα-syn*, but not pα-synF, was rabbit anti pS129 α-syn antibody GTX50222 from GeneTex, lot 821,505,177 (IF concentration 1/1000, IHC concentration 1/200, WB concentration 1/250). Other antibodies were rabbit anti phospho-acetyl-CoA carboxylase Ser79 from Thermo Fisher (IF concentration 1/150); rabbit anti BiP clone C50B12 from Cell Signaling Technologies (IF concentration 1/100); rabbit anti phospho-cJun Ser73 from Thermo Fisher (IF concentration 1/150); goat anti catalase from Novus Biological (IF concentration 1/150); mouse anti cytochrome C clone 6H2·B4 from BD Pharmingen (IF concentration 1/150); rabbit anti EEA1 clone C45B10 from Cell Signaling Technologies (IF concentration 1/100); mouse anti phospho-ERK1 Thr202/Tyr204 clone 4B11B69 from Biolegend (IF concentration 1/125); goat anti phospho-ERK5 Thr218/Tyr220 from Santa Cruz (IF concentration 1/200); chicken anti GFAP from Biolegend (IF concentration 1/4000); goat anti LAMP1 from R&D Systems (IF concentration 1/400); rabbit anti phospho-GSK3β Ser9 from Thermo Fisher (IF concentration 1/125); rabbit anti phospho-JNK1 + JNK2 + JKN3 Thr183/Tyr185 from Thermo Fisher (IF concentration 1/650, IHC concentration 1/200), chicken anti phospho-JNK Thr183/Tyr185 from Thermo Fisher (IF concentration 1/500); rabbit anti phospho MKK4 Ser80 from GeneTex (IF concentration 1/100); rabbit anti phospho MKK4 Thr261 from GeneTex (IF concentration 1/150); rabbit anti phospho MKK7 Ser271/Thr275 from Bioss (IF concentration 1/150); mouse anti NeuN clone A60 from EMD Millipore (IF concentration 1/150); rabbit anti phospho-p38 Thr180/Tyr182 from Thermo Fisher (IF concentration 1/250); mouse anti parkin (PRK8) from Santa Cruz Biotechnology (IF concentration 1/50); mouse anti phospho-Tau Ser202/Thr205 clone AT8 from Thermo Fisher (IF concentration 1/250); rabbit anti phospho-Tau Ser199 clone 2H23L4 from Thermo Fisher (IF concentration 1/100); mouse anti Tom20 clone 2F8.1 from EMD Millipore (IF concentration 1/75); rabbit anti tyrosine hydroxylase from Abcam (IHC concentration 1/750).

#### 2.1.2. Secondary antibodies

We used the following secondary antibodies from Jackson ImmunoResearch Laboratories: Alexa Fluor® 488-conjugated Donkey anti Rabbit IgG (H + L), Alexa Fluor® 488-conjugated Donkey anti Chicken IgG (H + L), Alexa Fluor® 594-conjugated Donkey anti Rabbit IgG (H + L), Alexa Fluor® 594-conjugated Donkey anti Mouse IgG (H + L), Alexa Fluor® 594-conjugated Donkey anti Goat IgG (H + L), Alexa Fluor® 594-conjugated Donkey anti Chicken Fab2 fragment IgG (H + L), Alexa Fluor® 647-conjugated Donkey anti Chicken IgG (H + L). Molecular Probes (Invitrogen) antibodies were: Alexa Fluor® 488-conjugated anti Mouse IgG (Fab2), Alexa Fluor® 647-conjugated anti Mouse IgG (Fab2), Alexa Fluor® 647-conjugated anti Rabbit IgG (Fab2), Alexa Fluor® 647-conjugated Donkey anti Goat IgG (H + L).

All secondary antibodies were used for IF at a concentration of 1/1500–1/2000.

### 2.2. Primary neuronal cultures and PFFs seeding

Primary neuronal cultures were prepared from E16-E18 C57BL/6J mouse brains (Charles River Laboratories) using standard procedures.

For immunofluorescence experiments, dissociated hippocampal or cortical neurons were plated onto poly-L-lysine coated glass coverslips placed in 24-well plates, at a cell density of 125,000 cells/well.

During plating, the cells were maintained in DMEM plus 10% horse serum and penicillin/streptomycin for 1 h. Thereafter, the medium was replaced and neurons were cultured in a serum free, neuron-specific, medium (Neurobasal® medium, N2, B27, sodium pyruvate and GlutaMAX®, Gibco). Cultures were maintained in a humidified 37 °C incubator with 5% CO2.

Neuronal cultures were seeded with PFFs at 5–6 days in vitro (DIV). Recombinant full length, wild-type α-syn PFFs were purified and prepared as described previously (Volpicelli-Daley et al., 2014b; Volpicelli-Daley et al., 2011). Briefly, α-syn PFFs were generated by incubating

purified α-syn (5 mg/ml in PBS) at 37 °C with constant agitation for 5 days, followed by the preparation of aliquots and storage at −80 °C. Just before seeding, PFFs were diluted in PBS at 0.1 mg/ml, sonicated during 30 s (0.5 s ON, 0.5 s OFF, power 30%), and diluted in neuronal media. Two μg/ml PFFs (final) per well were added on 24-well plates for immunofluorescence experiments. In the case of control conditions, an equivalent volume of PBS was added to the neuronal cultures.

Addition of α-syn monomers at a concentration of 4 μg/ml of monomer per well on 24-well plates was done as a control.

### 2.3. Immunofluorescence experiments

Neurons were fixed for 30 min at room temperature with 4% (*w/v*) paraformaldehyde in PBS containing 4% (w/v) sucrose. Neurons were washed with PBS, permeabilized with 0.2% (*v*/v) Triton X-100 in PBS for 6 min, washed again in PBS and blocked for 1 h at room temperature. After labeling with a first primary antibody (overnight at 4 °C) and washing with PBS, cells were incubated with an Alexa Fluor 488, 594 or 647 conjugated secondary antibody (1 h at room temperature in the dark) and washed with PBS, stained with DAPI and mounted on microscopy slides with ProLong Gold antifade reagent.

Assays involving the use of Mitotracker Red CMXRos were performed as follow. Cells were loaded with Mitotracker Red CMXRos at a concentration of 250 μM and incubated at 37 °C for 30 min. Thereafter, the cells were washed with PBS and fixed with 4% (*w/v*) paraformaldehyde in PBS containing 4% (w/v) sucrose for 30 min. Subsequent steps (blocking, labeling and mounting) were similar as described previously. Of note, MitoTracker Red CMXRos is a red-fluorescent dye that stains mitochondria in live cells and its subcellular colocalization requires the existence of a membrane potential.

### 2.4. Confocal microscopy

The cells were visualized using a spectral confocal microscope (Olympus FV1000). Images were captured and digitized using Olympus Fluoview Viewer software. Figs. 3, 4, 7 and supplementary Figs. 1, 2 and 3 are *Z*-stack reconstructions (of 4—6 confocal images). Other figures are composed of confocal images (0.2 μM). In some cases, the images were analyzed using ImageJ software. All images were processed using Adobe Photoshop.

### 2.5. Quantitative colocalization studies

Colocalization analysis was performed using the ImageJ plugin JACoP https://imagej.nih.gov/ij/plugins/track/jacop.html, (Bolte and Cordelieres, 2006). The Mander's colocalization coefficient (MCC) was used to measure the fraction of one protein colocalizing with another protein independently of the existence of a linear correlation between signal intensities (Dunn et al., 2011; Zinchuk and Grossenbacher-Zinchuk, 2014).

Statistical analyses were performed using the two-tailed *t*-test when two values were compared, and ANOVA for multiple comparisons (Prism v7).

### 2.6. Anisomycin treatment

Neurons were treated with anisomycin or the DMSO vehicle (A9789, Sigma) at a concentration of 25 μg/mL and incubated at 37 °C for 30 min. Following treatment, cells were washed with PBS and fixed with 4% (*w/v*) paraformaldehyde in PBS containing 4% (w/v) sucrose for 30 min. Subsequent steps (blocking, labeling and mounting) were similar as described previously.

### 2.7. Alpha-syn PFFs injections in mice

All animal experiments were performed in accordance with protocols approved by the Scripps Florida Institutional Animal Care and Use Committee (IACUC). Three months old male C57BL/6 J mice (Jackson Laboratories) weighing in the range of 25 to 30 g were used. They were randomly divided into two groups to receive saline ($n = 6$) or α-syn PFFs ($n = 6$). Mice were acclimated for 1 week prior to initiation of study, and then anesthetized via an intraperitoneal injection of ketamine and xylazine and placed into a stereotaxic frame (Stoelting). Unilateral injections (one single dose per animal) were made into the right side of mice striatum at stereotaxic coordinates AP +0.2 mm, ML +2.0 mm and DV -2.6 mm. A volume of 2.5 μl of saline containing α-syn PFFs at a concentration of 2 μg/μl or a corresponding amount of saline alone was injected with a 26-gauge Hamilton syringe and a motorized stereotaxic injector (Stoelting) at a rate of 0.5 μl/min. The needle was left in place for 5 min following each injection before retracting to prevent backfilling along the injection tract. Formation of α-syn aggregates was allowed to proceed for 30 days. At that point, brains were collected for IHC.

Animals were euthanized by an overdose of ketamine and xylazine, followed by cardiac perfusion with 0.9% saline and then with 4% paraformaldehyde. The brains were removed and further post-fixed in 4% paraformaldehyde at 4 °C for 1 day, followed by immersion on 30% sucrose (for cryoprotection) during 3 to 4 days. Brains were embedded and frozen in optimal cutting temperature (OCT) compound and stored frozen at −80 °C until sectioning. Symmetrical 40 μm thick sections were cut on a cryostat (Leica CM3050S) from +0.2 to −4.0 mm relative to the bregma, and some sections including portions of striatum or substantia nigra (~21–24 slices) were processed for IHC by the free-floating method. Briefly, free floating brain sections were placed into PELCO Prep-Eze™ 24 well plate mesh inserts (TedPella Inc.) under constant agitation and washed several times with TTBS 0.1% to remove excess of OCT and cryoprotectant. Then, samples were pretreated with 0.3% hydrogen peroxide for 15 min, washed with TTBS 0.1% and then blocked with 4% bovine serum albumin (BSA) for 1 h at room temperature. After labeling with a first primary antibody (overnight at 4 °C) and washing with TTBS 0.1%, brain sections were incubated with an Alexa Fluor 488 or 594 conjugated secondary antibody (2 h at RT in the dark) and washed again with TTBS 0.1%. Sections were mounted on Superfrost Plus slides, and a drop of Fluoroshield mounting medium with DAPI (1:4) was applied to each section. Slides were then sealed using coverslips and nail polish and stored at 4 °C.

It is noteworthy to mention that, for proper identification of the substantia nigra pars compacta (SNpc), some brain sections were incubated overnight at 4 °C with antibody against tyrosine hydroxylase (TH). Those slices adjacent to TH-positive sections were then selected to staining with for pS129 α-syn specific antibodies.

Brain sections were visualized using a spectral confocal microscope (Olympus FV1000). Images were captured and digitized using Olympus Fluoview Viewer software. In some cases, the images were analyzed using ImageJ software. All images were processed using Adobe Photoshop.

### 2.8. Postmortem human brain tissues

Fixed brain necropsies sections of frontal cortex of elderly subjects ranging from 65 to 90 years old were kindly donated by the National Brain and Tissue Resource for Parkinson's Disease and Related Disorders, Banner Sun Health Research Institute (Sun City, Arizona) - The Brain and Body Donation Program (BBDP) (http://www.brainandbodydonationprogram.org). Samples received included 40 μm free floating sections fixed in 4% buffered formaldehyde from 8 control patients, 8 PD patients classified as “low Lewy Bodies”, and 8 PD patients classified as “high Lewy Bodies”. Subjects were classified according to Braak's scoring from II to V. Non Parkinson's disease subjects were used as control cases in this study.

A standard protocol for the neuropathological evaluation of all BBDP autopsied brains was used (with slight modifications). Briefly,

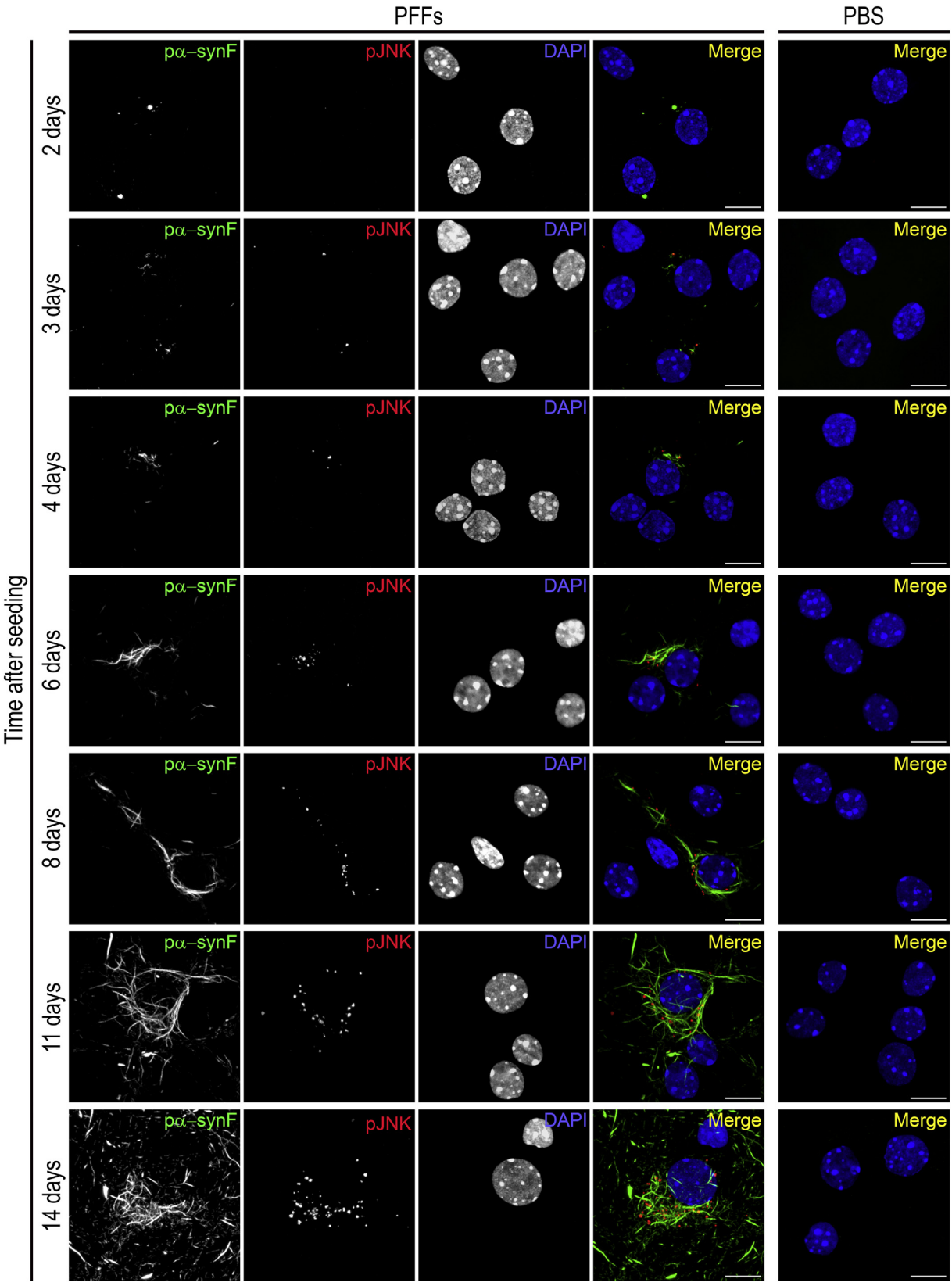


**Fig. 1.** Time-course of appearance of pJNK inclusions in PFF-seeded neurons.
Primary hippocampal mouse neurons were exposed to preformed fibrils (PFFs) at DIV7 and examined by ICC at various time points from day 2 to 14. Cells similarly treated with PBS alone constitute the control. Pictures show labeling for pα-synF and pJNK in green and red, respectively, and DAPI staining in blue for the nuclei. Neurons from the PBS control were labeled similarly, the merged image is shown. No pJNK signal was observed in control cells in our experimental conditions. Scale bars = 10 μm.

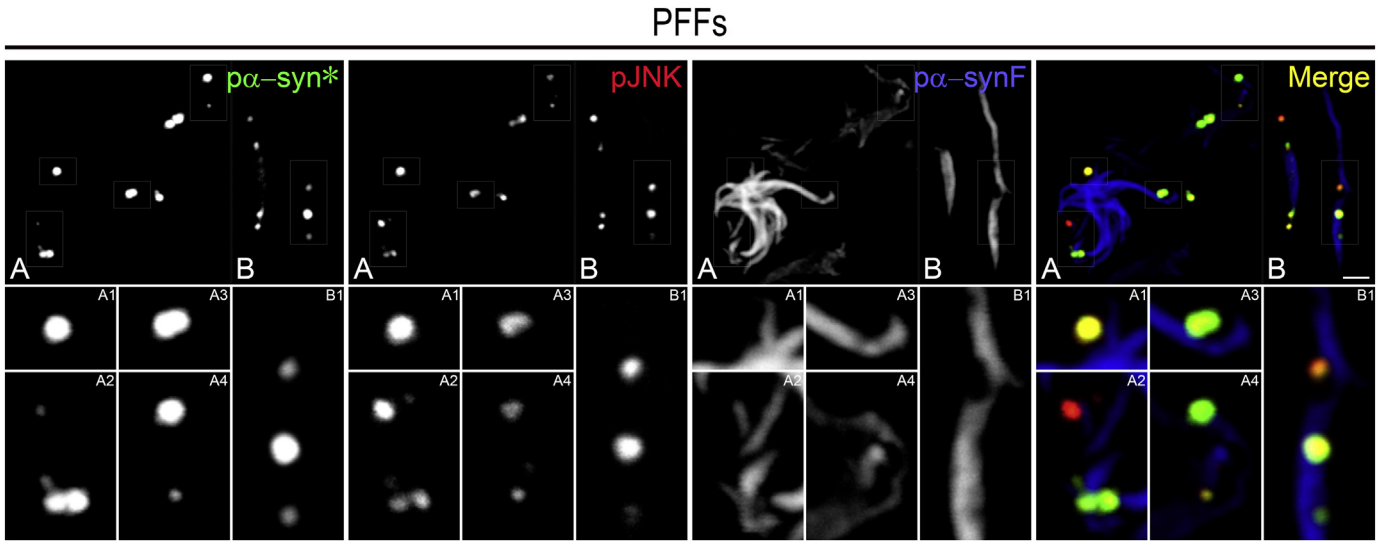


**Fig. 2.** pJNK colocalizes with pα-syn* but not pα-synF.
pJNK positive inclusions coincide completely with pα-syn* inclusions. The intensity of the staining may vary, leading to inclusions exhibiting a predominance of green or red in the merged image. On the other hand, pα-synF antibody labeled fibrillary structures that excluded pJNK labeling. In insets A1 and B1, several indents in pα-synF labeling can be seen, corresponding to the formation of pα-syn* from partial digestion of pα-synF (Grassi et al., 2018). Pictures show labeling for pα-syn*, pJNK and pα-synF in green, red and blue respectively. Scale bars = 5 μm.

40 μm thick free floating brain sections were sectioned in small pieces, placed into PELCO Prep-Eze™ 24-well plate mesh inserts (TedPella Inc.) under constant agitation and washed several times in PBS plus Triton X-100 0,1% in PBST 0,1% to remove the cryoprotectant. Thereafter, sections were incubated with formic acid 70% at 37 °C for 10 min (antigen retrieval), washed again with PBST 0,1% and then blocked with horse serum 10% at room temperature for 2 h. After labeling with a first primary antibody (overnight at 4 °C) and washing with PBS, sections were incubated with an Alexa Fluor 488 or 594 conjugated secondary antibody (2 h at room temperature in the dark) and washed with PBS, stained with DAPI and mounted on microscopy slides plus coverslips with ProLong Gold antifade reagent and stored at 4 °C.

Brain sections were visualized using a spectral confocal microscope (Olympus FV1000). Images were captured and digitized using Olympus Fluoview Viewer software. In some cases, the images were analyzed using ImageJ software. All images were processed using Adobe Photoshop.

## 3. Results

### 3.1. Early appearance of pJNK positive inclusions

Our objective was to determine which molecular pathway(s) are involved in the mitochondrial toxicity induced by pα-syn*. Since JNK phosphorylation has been shown in the brains of PD patients and in PD mouse models (Ferrer et al., 2001; Hunot et al., 2004) we first labeled PFF-exposed primary mouse neurons with an antibody against pJNK. pJNK labeling appeared as small inclusions present as early as 2 days after seeding, the number of which progressively increased in the culture in a manner highly reminiscent of pα-syn* propagation (Grassi et al., 2018) (Fig. 1). No pJNK labeling was detected after exposure of primary neurons to monomeric α-syn (Fig. S1). pJNK labeling was specific to neuronal cells (Fig. S2). Of note, by “pJNK labeling”, we describe pJNK labeling found exclusively in PFF-treated neurons in experimental conditions where physiological axonal pJNK was not detected, i.e. the concentration of pJNK antibodies used was appropriate for the detection of somatic pJNK aggregates without significant staining of the physiological levels of axonal pJNK.

### 3.2. pJNK positive inclusions correspond to pα-syn* aggregates

pJNK inclusions tightly co-localized with small pα-syn* aggregates, but not pα-synF fibrils (Fig. 2). Pα-syn* and pα-synF are recognized by two different α-syn antibodies. Pα-syn*/JNK labeling and pα-synF labeling were mutually exclusive. As described previously (Grassi et al., 2018), pα-syn* inclusions were released from pα-synF, with pJNK being present in pα-syn* positive inclusions as early as these were observable. Fig. 2 A1 & B1 show several indents in pα-synF fibers, with the presence of newly formed pJNK positive pα-syn* aggregates.

### 3.3. JNK is also activated in brains of PFF-injected mice and PD patients

We observed pJNK positive inclusions in the brains of mice stereotaxically injected with PFFs and in PD patients brains, confirming the biological relevance of the findings in primary neuronal cultures (Fig. 3 and Fig. S3).

### 3.4. Pα-syn* inclusions triggers phosphorylation of several members of the MAPK family of kinases

pJNK activation was not related to canonical Jun phosphorylation (Fig. 4). We further observed that other members of the MAPK family of kinases were phosphorylated in pα-syn* inclusions (Figs. 5 and 10). The activated form of MKK4, a kinase that activates JNK and p38 (Cuenda, 2000), exhibited tight colocalization with pJNK. Abundant T261-phosphorylated (activated) MKK4 was present in pα-syn*/pJNK inclusions (Fig. 5A), contrasting with very rare S80-phosphorylated (inactivated) (Crittenden and Filipov, 2011) MKK4 (Fig. 5B), indicating that pα-syn* was associated with the accumulation of the activated, but not the inactivated form of the enzyme. Phosphorylated p38 was also co-localizing with pα-syn*/pJNK inclusions, as well as pERK5 (Fig. 5C-D). On the contrary, pMKK7 and pERK1/2 did not colocalize with pα-syn*/pJNK inclusions (Fig. S4), and pGSK3β, a kinase not belonging to the MAPK pathway, exhibited partial colocalization (Fig. 5E).

### 3.5. Pα-syn* inclusions are associated with ptau aggregates

Oligomeric ptau aggregates have been described at the mitochondria, and it has been suggested that these represent a toxic form of tau

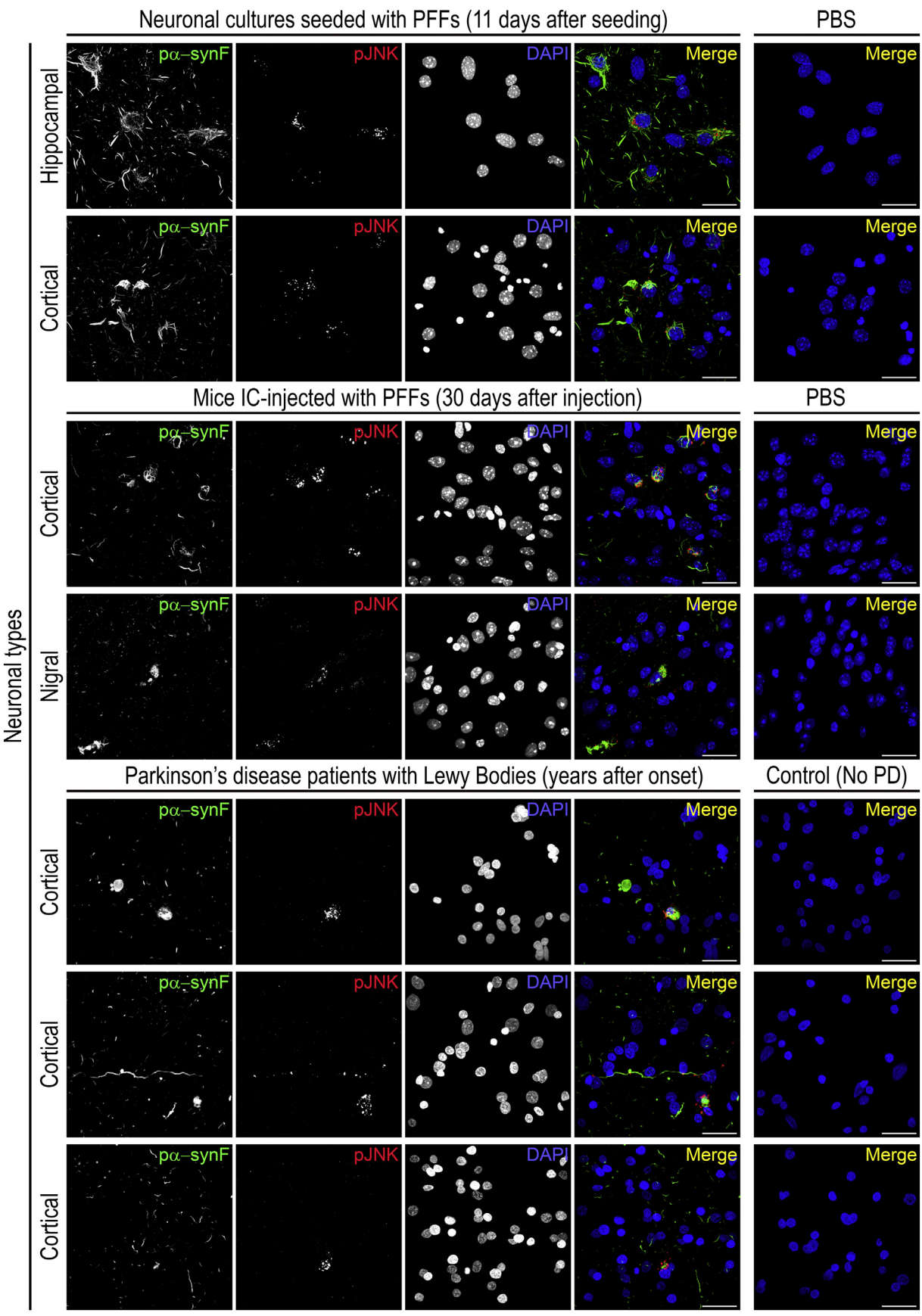


*(caption on next page)*

**Fig. 3.** Detection of pα-synF and pJNK positive inclusions in the brains of PFF-injected mice and PD patients.
Upper panels: Mouse hippocampal or cortical primary neurons seeded with PFFs develop pα-synF aggregates and pJNK positive inclusions. Middle panels: Mice stereotaxically injected with PFFs in the striatum develop pα-synF aggregates and pJNK positive inclusions in the cortex and substantia nigra, with morphologies and subcellular localization identical to the cell cultures. Lower panels: pα-synF aggregates and pJNK positive inclusions were observed in the cortex of 3 LB positive patients with PD. The LBs are detected using the pα-synF specific antibody. Pictures show labeling for pα-synF, pJNK and nuclear DAPI staining in green, red and blue, respectively. Scale bars = 20 μm.

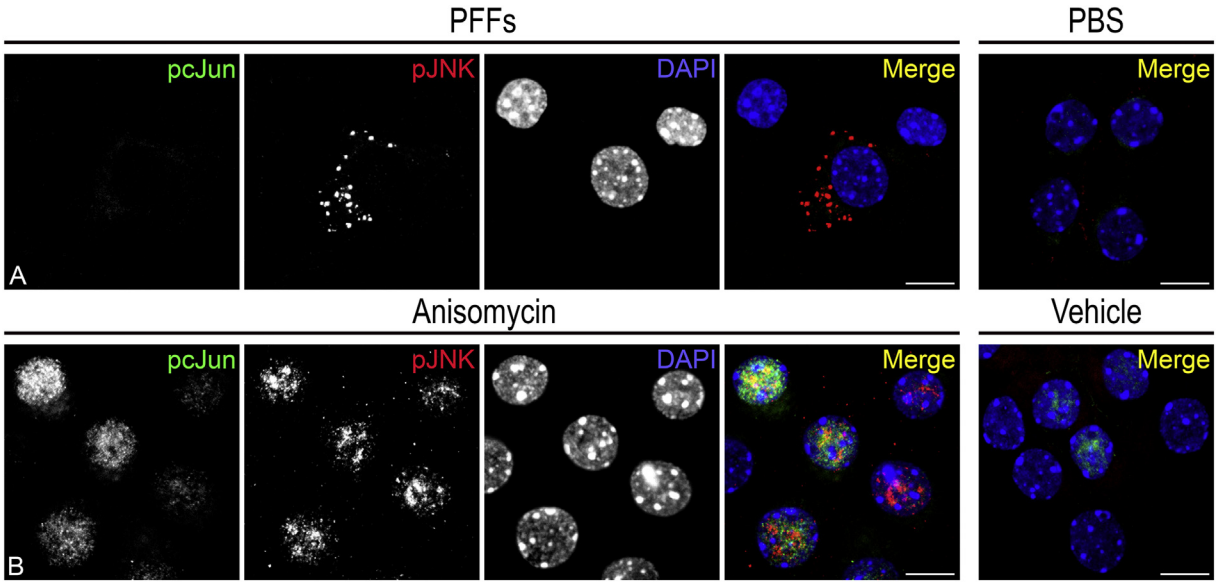


**Fig. 4.** PFF seeding induces non-canonical JNK activation.
A. PFFs-seeded neurons accumulate pJNK in the extranuclear but not the intranuclear compartment, and do not accumulate pcJun. B. Neurons treated with anisomycin, a compound known to activate the canonical pathway of JNK and used herein as a positive control, exhibit pJNK as well as pcJun labeling in the nucleus. A-B. PBS treated control cells exhibit faint basal pcJun labeling detectable in some, but not all, nuclei. Pictures show labeling for pcJun, pJNK and nuclear DAPI staining in green, red and blue respectively. Scale bars = 10 μm.

(Lasagna-Reeves et al., 2011). Moreover, tau pathology is found in PD patients and animal synucleinopathy models (Haggerty et al., 2011; Irwin et al., 2013; Sengupta et al., 2015), and tau is a substrate for phosphorylation by several MAPK proteins (Martin et al., 2013). We therefore investigated if pα-syn*, via the tightly associated activated kinases identified above, might be the culprit in triggering tau phosphorylation, by co-immunolabeling for pJNK and/or pα-syn*, and ptau. While pα-syn* and pJNK were completely colocalizing (Fig. 6A), pα-syn* and ptau aggregates were either largely overlapping (Fig. 6B&D) or juxtaposed (Fig. 6C&D). These observations suggest that pα-syn* triggers MAPKs phosphorylation, and that activated MAPKs then induce tau phosphorylation and aggregation in the vicinity of pα-syn*.

### 3.6. Pα-syn*/ptau aggregates colocalize at damaged mitochondria

In Fig. 2, we demonstrated that JNK was activated in early pα-syn* aggregates shed from pα-synF fibrils. In Fig. 7, we show that pJNK was still associated with mature pα-syn* aggregates localized to the mitochondria. pJNK/pα-syn* inclusions colocalized with Tom20, a marker of the outer mitochondrial membrane, but pα-synF did not. Fig. 7C-E depicts highly fragmented mitochondria in areas of abundant pα-syn*/pJNK inclusions. Similar to what we described for pα-syn* (Grassi et al., 2018), pJNK labeling colocalized exquisitely with areas of mitochondrial damage as shown in Fig. 8 by the following 1) loss of membrane potential (Fig. 8A), 2) pACC1 sequestration (Fig. 8B, Fig. S5B), 3) cytochrome C staining (Fig. 8C, Fig. S5A). Colocalization with BiP, a resident protein of mitochondria associated ER membranes (MAMs), indicates that pα-syn*/pJNK inclusions occur at MAMs (Fig. 8C, Fig. S5C). Mitotracker CMXRos labeling, a marker of mitochondrial potential, was missing in the direct vicinity of pJNK punctae (Fig. 8A). Pα-syn* and ptau were both found surrounded by abundant cytochrome C staining at the mitochondria (Fig. 8D), supporting previous suggestions that ptau contributes to mitochondrial toxicity in synucleinopathies. We found a small proportion of pJNK positive aggregates juxtaposed to catalase positive peroxisomes (Fig. S5). No colocalization was found with EEA1 positive early endosomes (Fig. S5).

### 3.7. Pα-syn*/ptau aggregates are associated with mitophagy

We previously showed that pα-syn* induced mitochondrial fragmentation and mitophagy. Here, we observed that pJNK positive inclusions colocalized with Tom20 in parkin-positive LAMP1 vesicles (Fig. 9A-B, Fig. 9A also shows fragmented mitochondria), showing that pa-syn*/pJNK-bearing mitochondria underwent mitophagy. pTau colocalized with pJNK inclusions in mitophagic vesicles (Fig. 9C-D).

### 3.8. Quantitative colocalization

Ninety percent of pα-syn* staining co-localized with pJNK staining, and vice-versa (Fig. 10A). Importantly, nearly all pα-syn* inclusions (and all pα-syn* positive neurons) were positive for pJNK. At times, pJNK staining in a given inclusion was more intense than pα-syn* staining, or inversely pα-syn* was more intensely stained than pJNK (shown in Fig. 2). Colocalization reached comparable levels with activated pMKK4, pp38 and pERK5, but not pGSK3β (Fig. 10A).

pJNK/pα-syn* inclusions did trigger extremely few phosphorylation events of MKK4 at the inhibitory site S80, hence the poor colocalization of pJNK with pMKK4 (S80) (red bars); however, the few positive pMKK4 (S80) dots were colocalizing with pJNK (green bars). The difference in colocalization of pJNK with either pMKK4 (T261) or pMKK4 (S80) was highly significant statistically.

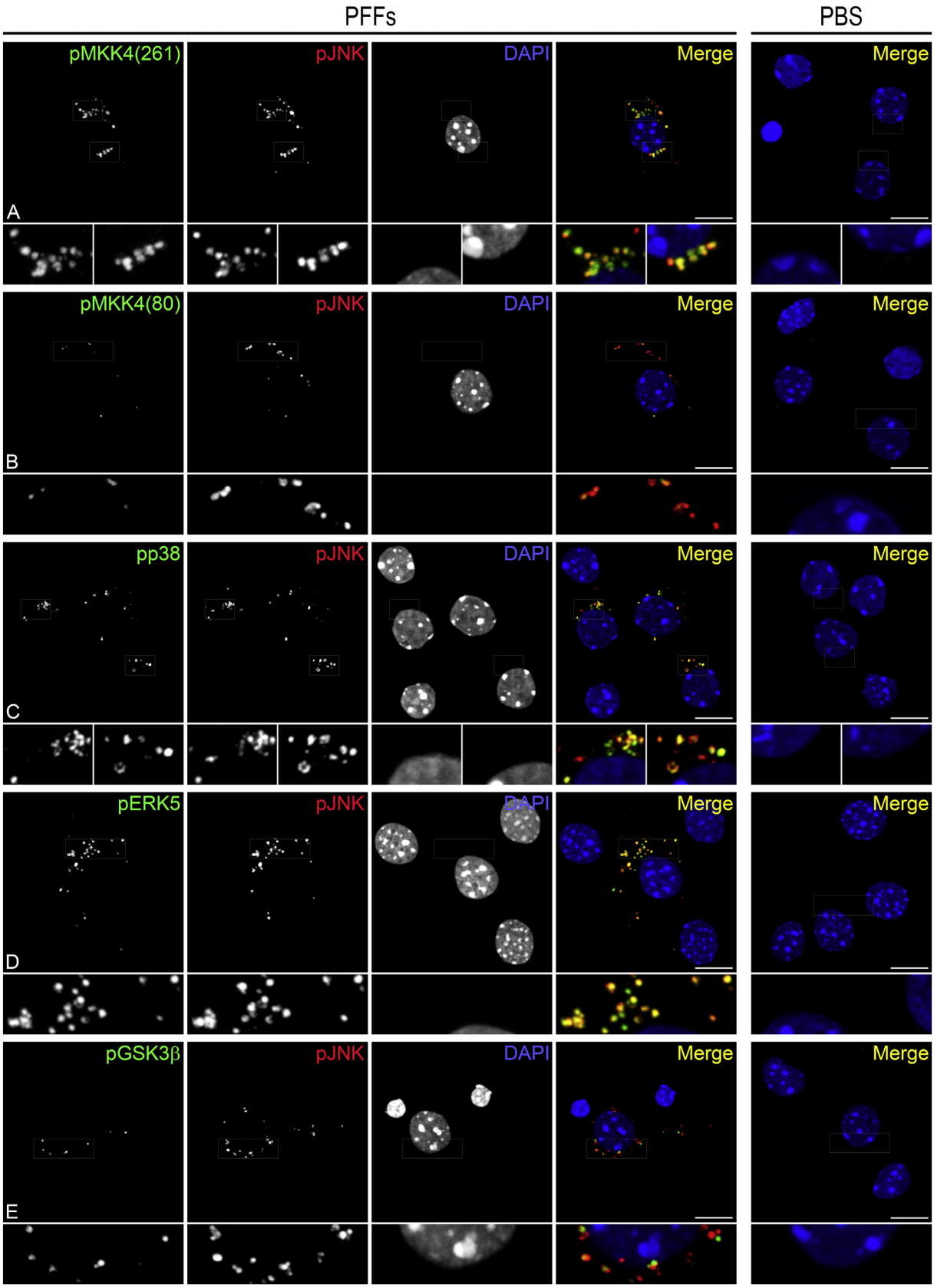


**Fig. 5.** P-αsyn* induces MAPK pathway activation.
A. pJNK positive inclusions colocalize with MKK4 phosphorylated at T261 (activated MKK4). B. Very few dots corresponding to MKK4 phosphorylated at S80 (inactive MKK4) are detected, however pMKK4 (T80) positive dots colocalize to pJNK positive inclusions. C-D. pp38 and pERK5 labelling largely overlaps with pJNK positive inclusions. E. pGSK3β positive dots are detected in close proximity to pJNK positive inclusions with no or only partial overlap. Cells were labeled with phosphorylation-site specific pMKK4, pGSK3β, pp38 or pERK5, and pJNK antibodies and DAPI, color-coded respectively as green, red and blue in the merged image. Scale bars = 10 μm.

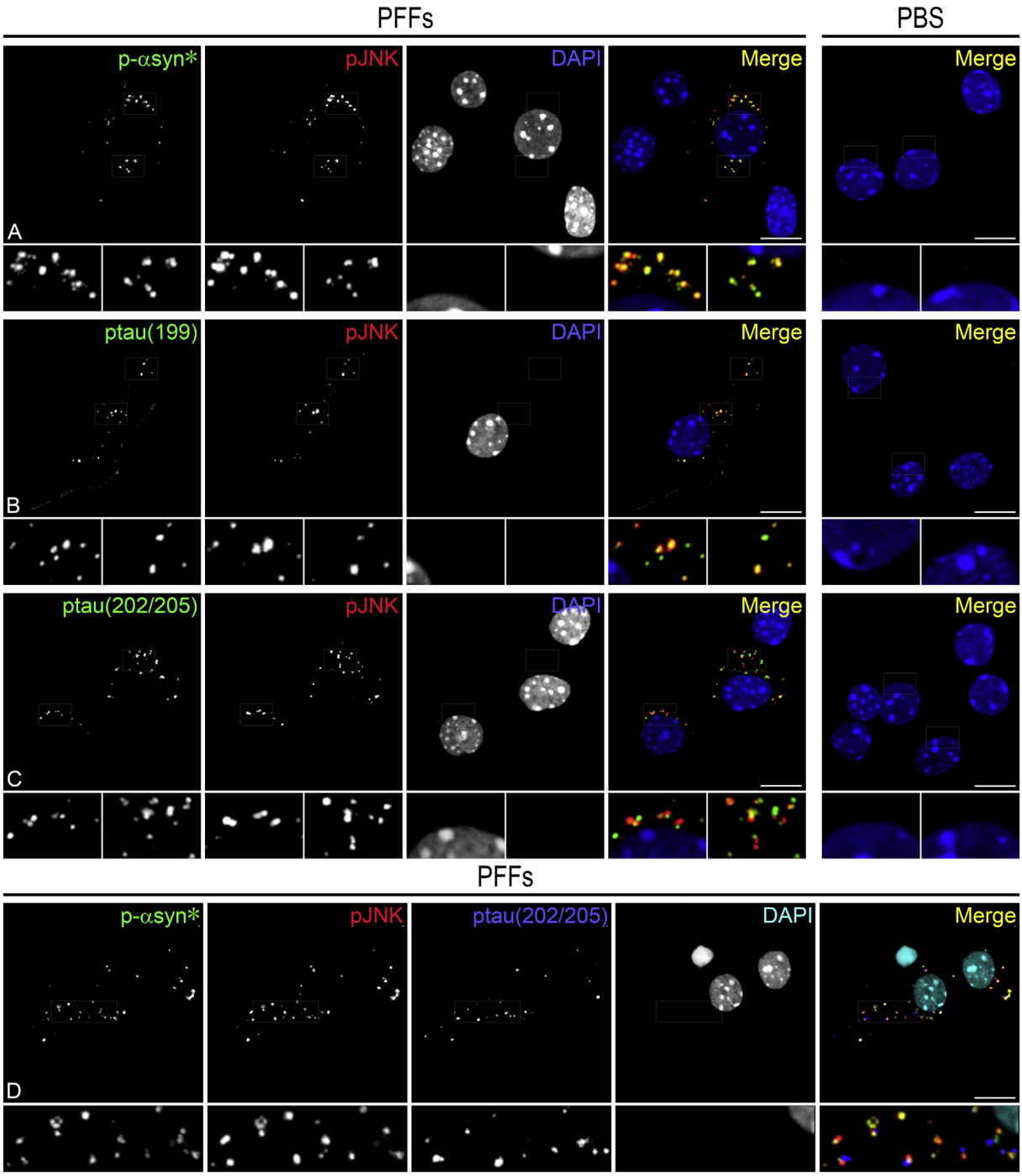


**Fig. 6.** P-αsyn* aggregates co-localize with ptau aggregates.
A. pJNK localizes to pα-syn* inclusions. B–C. pTau positive inclusions were juxtaposed with or colocalized with pJNK positive inclusions. This was found with both ptau antibodies used, targeting either pS199 (B) or pS202/T205 (C). D. Triple labeling showing the colocalization of pα-syn* and pJNK, with ptau inclusions being either colocalized or directly juxtaposed. A-D. Cells were labeled with phosphorylation-site specific ptau or pα-syn*, and pJNK antibodies as well as DAPI staining, color-coded respectively as green, red and blue in the merged images. Scale bars = 10 μm.

Finally, about 60% colocalization was found between pα-syn*/pJNK positive aggregates and ptau, consistent with the observation of both protein aggregates being juxtaposed or colocalizing (Fig. 10 A&B). Occasionally, pα-syn* inclusions were found without ptau. However, ptau was always seen colocalizing with pα-syn* aggregates. In our view, the most logical interpretation for these findings is that pα-syn* activates kinases that then phosphorylate tau. The phosphorylation cascade as well as the recruitment of tau by pα-syn* are not yet established in early pα-syn* aggregates, hence the presence of some pα-syn* aggregates in the absence of ptau. This cascade of events is described in Fig. 11.

Fig. 10C shows that 80% of pα-syn* and pJNK co-localize with LAMP1, in accordance with the fact that pα-syn* is found abundantly in mitophagic vesicles. Close to 70% of ptau colocalized with LAMP1. Parkin did not associate directly with pα-syn* inclusions (30% colocalization with pα-syn*, ptau or pJNK). A lower degree of colocalization of protein aggregates with parkin is to be expected since parkin ubiquinates outer mitochondrial membrane proteins to trigger selective

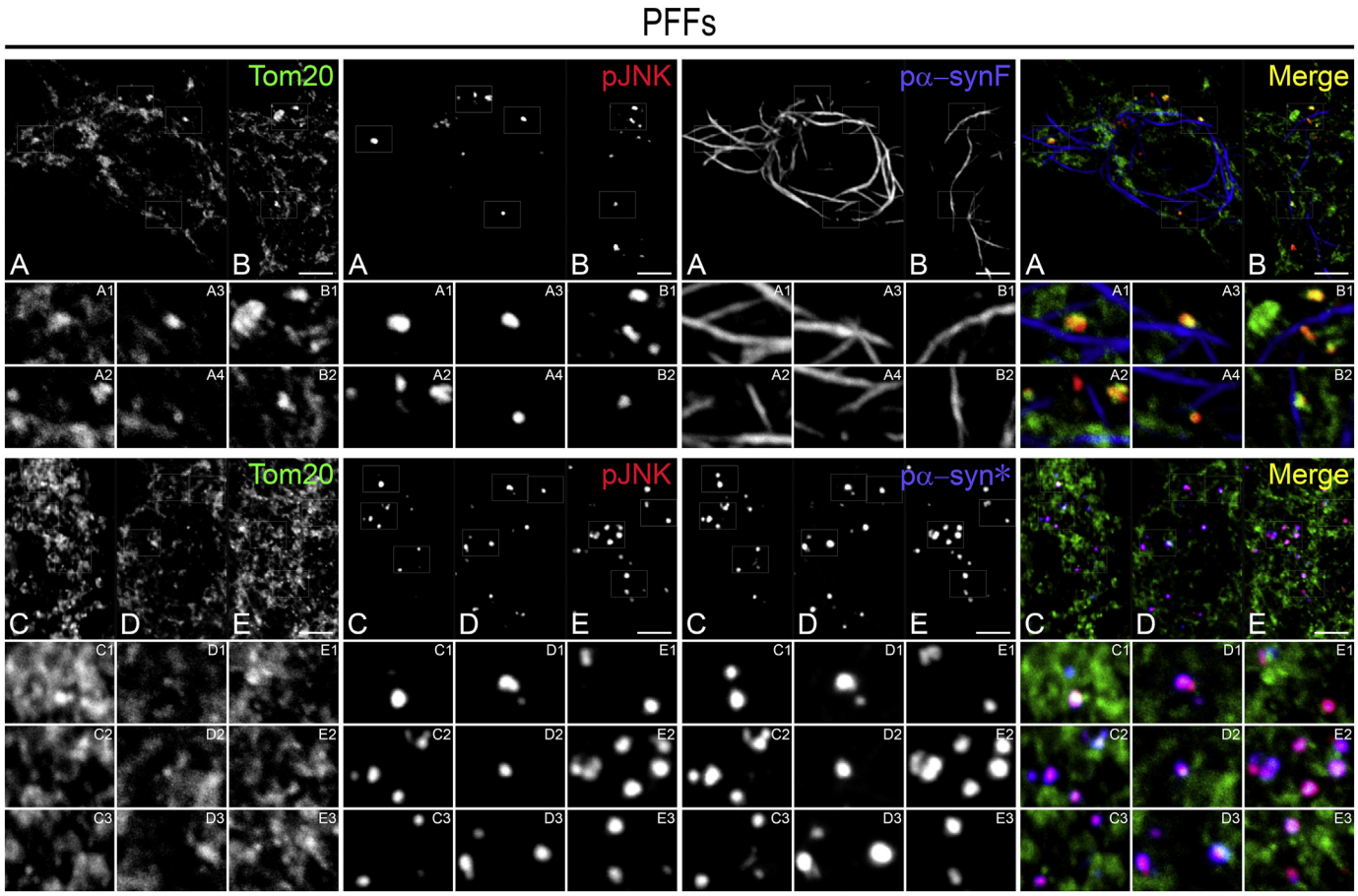


**Fig. 7.** pJNK colocalizes with pα-syn* at the mitochondrial membrane.
A-B. pJNK positive inclusions, but not pα-synF fibers, colocalize with Tom20, indicating their association with mitochondrial membranes. C-E. pJNK positive pα-syn* aggregates colocalize with Tom20. Pictures show cells containing abundant pα-syn* aggregates, associated with a fragmented mitochondrial network. Pictures show labeling for Tom20, pJNK, pα-synF or pα-syn*, and nuclear DAPI staining in green, red and blue respectively. Scale bars = 5 μm.

autophagy as a response to mitochondrial damage and PINK1 accumulation at the outer membrane (Pickrell and Youle, 2015).

## 4. Discussion

We recently identified pα-syn*, a conformationally distinct, small aggregate of pα-syn, resulting from incomplete autophagic degradation of Lewy body type pα-syn fibrils (pα-synF). After exiting autolysosomes, pα-syn* attaches to mitochondrial tubules, inducing metabolic stress, membrane depolarization and mitochondrial fragmentation. Pα-syn* is finally localized in mitophagic vacuoles surrounded by mitochondrial debris (Grassi et al., 2018).

In the present study, we defined some key molecular actors in the toxic pathway elicited by pα-syn*. Strikingly, we observed 80–90% colocalization of pα-syn* with phosphorylated JNK (pJNK, Figs. 2, 6 and 10). pJNK colocalized with pα-syn* early, i.e. as soon as pα-syn* was released from pα-synF, and was completely excluded from pα-synF (Figs. 1&2). Therefore, in some experiments, pJNK was used as a surrogate marker for pα-syn* aggregates. The pα-syn*/pJNK aggregates also colocalized with phosphorylated MKK4, a MAP kinase kinase (MAPKK) phosphorylating and activating JNK and p38 (Cuenda, 2000) (Figs. 5 and 10). Pα-syn* led to MKK4 phosphorylation overwhelmingly at its activation site T261 (as opposed to S80 leading to the inactivation of the kinase). We also found pα-syn*/pJNK aggregates colocalizing with pp38. On the contrary, MKK7, the second JNK-activating MAPKK, was not found to be phosphorylated in the vicinity of pα-syn* (Fig. S4). Altogether, these data strongly suggest molecule- and site-specific activation of MKK4 by pα-syn*, with pMKK4 then activating JNK and p38. We also found a high degree of colocalization of pα-syn* with pERK5, a MAPK of the MKK5/ERK5 pathway previously found to be activated in pα-syn aggregates bearing neurons (Volpicelli-Daley et al., 2014a).

pERK5 is involved in the regulation of energy metabolism. Indeed, ERK5 is activated and partially co-localized to mitochondria when oxidative phosphorylation is increased in leukemia cells (Charni et al., 2010). ERK5 has also been found to regulate mitochondrial function in cardiomyocytes (Liu et al., 2017). In cultured neurons, it has been suggested that ERK5 activation is involved in neuroprotective 'preconditioning' in the presence of reactive oxygen species (Su et al., 2014). The JNK family of kinases comprises 3 members. JNK1 and 2 are ubiquitously expressed, whereas JNK3 is expressed mostly in the brain (Yamasaki et al., 2012). P38 and JNK3 are phosphorylated in the brains of PD patients (Ferrer et al., 2001; Hunot et al., 2004). JNK3 is also increased in human cases of Alzheimer's disease and is involved in $A\beta_{42}$ production (Yoon et al., 2012). Both *Jnk2* and *Jnk3* knockout (KO) in mice is protective against acute 1-methyl-4-phenyl-1,2,3,6-tetrahydropyridine (MPTP) intoxication compared to both wild type and *Jnk1* knockout mice, manifested as a 3-fold increase of the number of TH-positive neurons (Hunot et al., 2004). JNK inhibitors have been shown to protect dopaminergic neurons in toxin models of PD in rodents (Chambers et al., 2011; Choi et al., 2010; Pan et al., 2015; Wang et al., 2004; Xia et al., 2001). P38 is involved in MPTP-induced neurotoxic signaling and is phosphorylated in mice expressing A53T α-syn (Ray et al., 2015; Wu et al., 2016; Chen et al., 2018). Therefore, our data suggest that activation of the MAPK pathway is directly involved in the mitotoxic effects of pα-syn*.

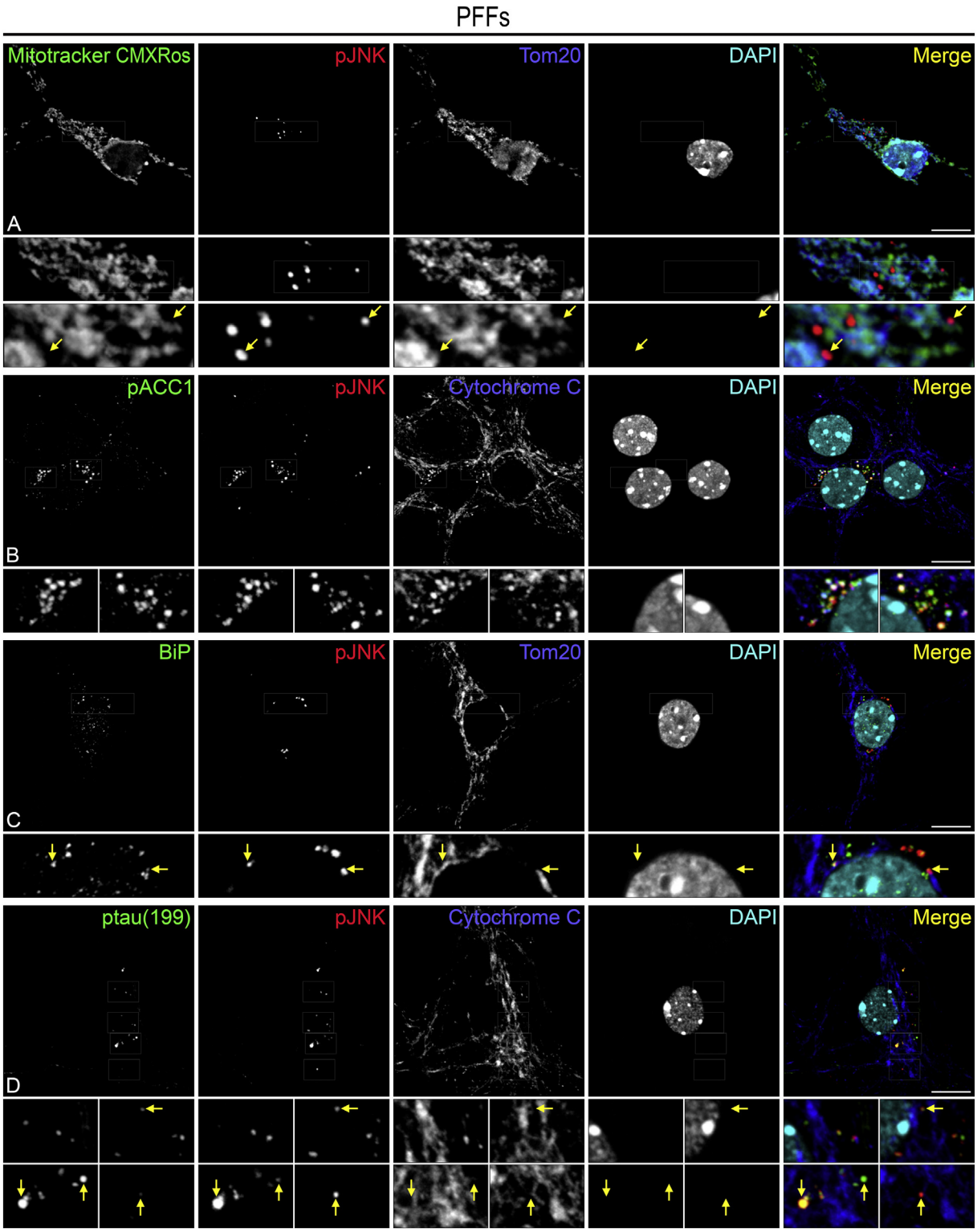


**Fig. 8.** pTau colocalizes with pJNK positive pα-syn* aggregates in areas of mitochondrial damage.
A. Mitotracker CMXRos staining is absent at the sites of mitochondrial attachment of pJNK positive inclusions. Arrows indicate Tom20 positive areas with interrupted Mitotracker CMXRos staining. B. pJNK positive inclusions colocalize with pACC1 and cytochrome C at the mitochondrial membrane. C. pJNK positive inclusions colocalize with BiP and Tom20, indicating their localization to mitochondria associated ER membranes (MAMs, arrows). D. Colocalization of pJNK positive inclusions and ptau occurs at areas of cytochrome C accumulation indicating damaged mitochondria (arrows). Pictures show labeling for Mitotracker CMXRos/pACC1/BiP/ptau, pJNK, Tom20/cytochrome C and nuclear DAPI staining in green, red, blue and turquoise, respectively. Scale bars = 10 μm.

Tau pathology has been shown to co-exist with α-synuclein pathology in the brains of PD and DLB patients as well as in rodent models of synucleinopathy; however the causal relationship between these aggregates has remained enigmatic (Haggerty et al., 2011; Irwin et al., 2013; Sengupta et al., 2015). PFFs are able to induce the formation of tau aggregates in cell culture (Guo et al., 2013), and α-synuclein binds tau directly via its acidic C-terminal domain (Kawakami and Ichikawa, 2015). We searched for ptau aggregates, and found them directly

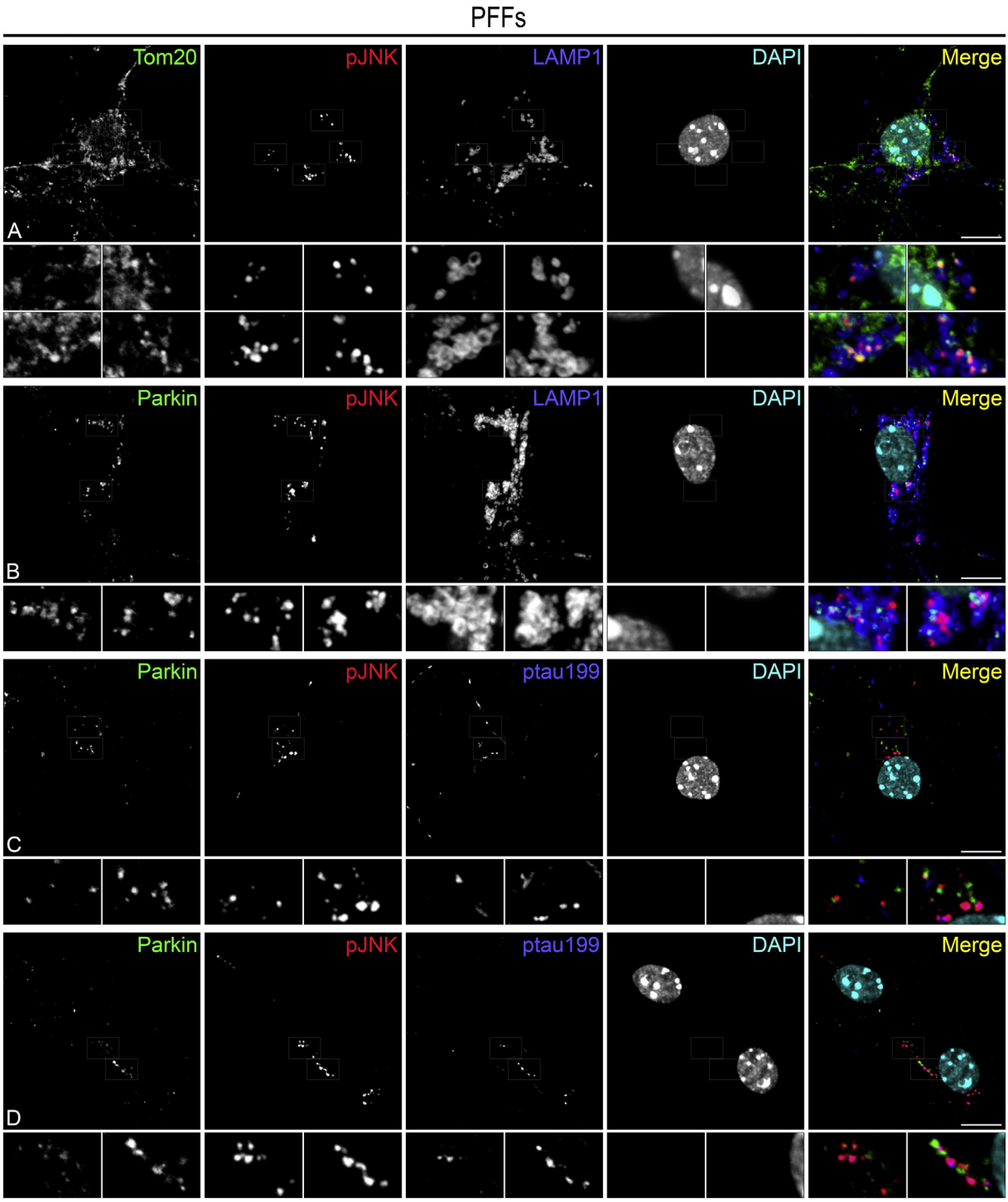


**Fig. 9.** pJNK positive pα-syn* aggregates and ptau co-localize in mitophagic vacuoles.
A. LAMP1 positive vesicles contain pJNK and Tom20 staining showing that they are mitophagic vacuoles. B. Parkin labeling is associated with pJNK positive inclusions in LAMP1 positive vesicles. C, D. pJNK positive pα-syn* aggregates colocalize with ptau and with parkin. Pictures show labeling for Tom20 or parkin, pJNK, LAMP1 or ptau and nuclear DAPI staining in green, red, blue and turquoise, respectively. Scale bars = 10 μm.

juxtaposed and/or overlapping with pα-syn* aggregates (Fig. 6). The pα-syn*/ptau aggregates were located at the mitochondrial membrane, specifically in areas of mitochondrial damage (shown by exquisite loss of mitotracker CMXRos labeling in the vicinity of pα-syn*; clustering of pACC1 that is a marker of energy deficit and mitochondrial membranes structural damage; cytochrome C accumulation; co-localization with BiP, a resident protein of MAMs that are recruited to initiate mitophagy, see Fig. 8). A large proportion of pα-syn*/ptau aggregates were found in LAMP-1 mitophagic vacuoles (Figs. 9 &10). These data suggest that pα-syn* and ptau act in concert to induce mitochondrial dysfunction. Consistent with this hypothesis, it has been previously proposed that mitochondrial tau inclusions are toxic. Tau oligomers localized to mitochondria after injection in mouse brains, inducing reduction of complex I (Lasagna-Reeves et al., 2011). pTau has been shown to interact with Drp1 leading to enhanced mitochondrial fission (Manczak and Reddy, 2012). The contribution of tau oligomers to neurotoxicity in

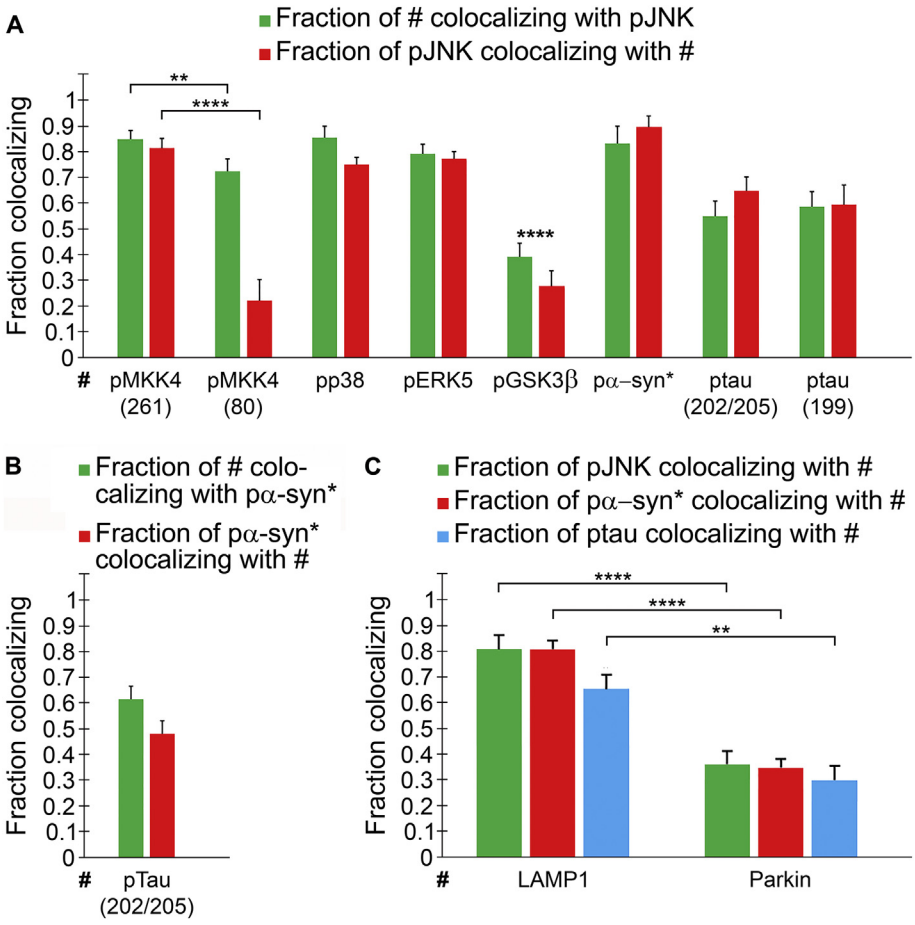


**Fig. 10.** Quantitative colocalization studies.
A. Graphs showing Manders' correlation coefficients of pJNK with pα-syn*, ptau and other kinases. pJNK labeling tightly associates with pα-syn* labeling, but also pMKK4 (activated), pERK5 and pp38 (≥80% colocalization). B. Graph showing Manders' correlation coefficient of pα-syn* with ptau. C. Graphs showing Manders' correlation coefficients of pα-syn*, pJNK and ptau with LAMP1 and parkin. A-C: Key to statistical analyses: $**p < .01$; $***p < .001$; $****p < .0001$. In A, **** without a bar indicates $p < .0001$ for pGSK3β colocalizing with pJNK significantly less than pMKK4, pp38 and pERK5 colocalize with pJNK. In C, p was 0.05 for the difference between ptau colocalization with LAMP1 and pa-syn*/pJNK colocalization with LAMP1.

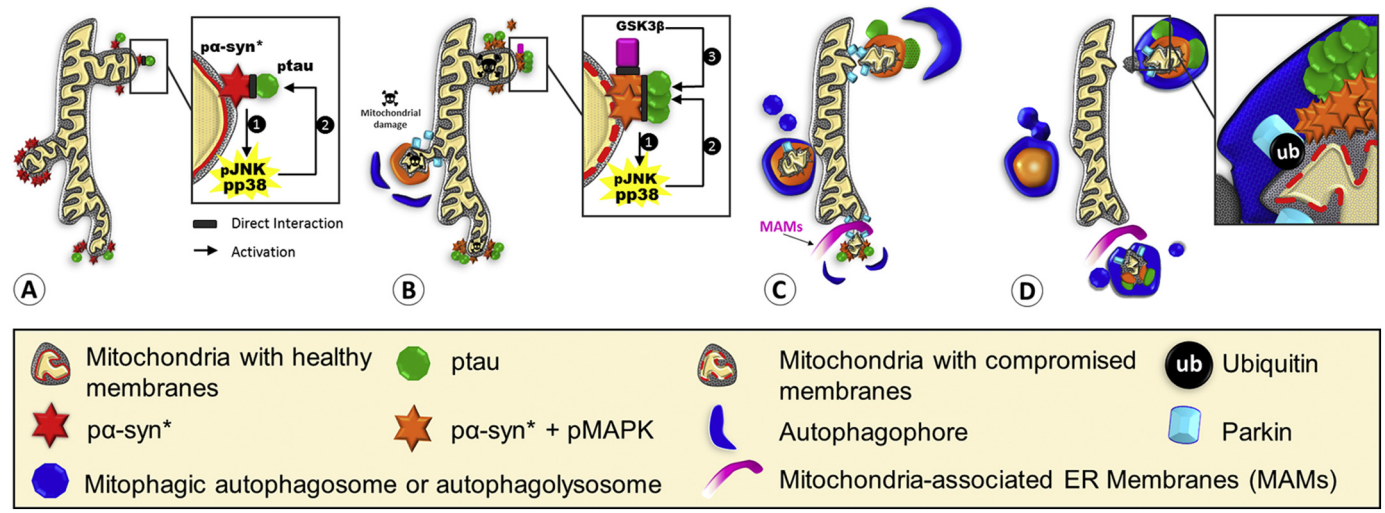


**Fig. 11.** Model for the molecular cascade and Tau recruitment induced by pα-syn*, leading to mitochondrial damage and mitophagy.
A. Pα-syn* aggregates associate to the mitochondrial membrane, triggering MAPK activation. Pα-syn* binds tau that is phosphorylated by these MAPKs. B. Both pα-syn* and ptau aggregates grow in size and induce mitochondrial damage. GSK3β, which is known to bind to α-syn, contributes to tau phosphorylation in cooperation with MAPKs. C. Pα-syn*/ptau aggregates induce mitochondrial fragmentation and recruit parkin, initiating mitophagy. D. Mitophagic vacuoles contain mitochondrial debris, along with pα-syn*/ptau/MAPK aggregates.

PD is also supported by the finding that the administration of an antibody directed against oligomeric tau ameliorated the neuropathological and disease phenotype in the transgenic A53T α-syn mouse model of PD (Gerson et al., 2018). Emphasizing the cooperation of pα-syn* and ptau in mitochondrial toxicity, fragmentation and mitophagy induction, we show that pα-syn*/pJNK/ptau inclusions are colocalizing with Tom20 (marker of the mitochondrial membrane) in parkin decorated, LAMP1 positive mitophagic lysosomes (Fig. 9 &10).

How does tau get phosphorylated?

Tau is a substrate for p38, JNK and GSK3β. P38 phosphorylates tau at 21 putative tau phosphorylation sites, among which 15 are phosphorylated in the brains of Alzheimer's disease (AD) patients (Martin

et al., 2013). JNK phosphorylates tau at 12 sites, all found phosphorylated in AD patients brains (Martin et al., 2013). GSK3β phosphorylates tau at 42 sites, among which 29 are found in AD brains, and p38 also phosphorylates GSK3β (Martin et al., 2013). We found tau to be phosphorylated at least at the S202/T205 cluster, which could be due to GSK3β, P38 or JNK (Duka et al., 2013). Tau is extensively modified in vivo by JNK at several conserved sites (Chang et al., 2003). For instance, in the FBW7 phosphodegron of tau (KKVAIIRTPPKSPA), T231 and S235 are phosphorylated by JNK in cooperation with GSK3 (Alonso et al., 2010; Cho and Johnson, 2004). JNK indeed acts as a "master" kinase for GSK3β (which is a "slave" kinase), meaning that some motifs on the enzyme's substrates need to be primed by JNK phosphorylation, turning on GSK3β phosphorylation at those sites (Sutherland, 2011). On the other hand, α-synuclein binds GSK-3β, leading to the autophosphorylation of the kinase that also phosphorylates tau at S396 (Kawakami and Ichikawa, 2015).

In the light of this knowledge, we interprete our data as follows (Fig. 11). Pα-syn* activates MKK4, leading to JNK and p38 activation, with both phosphorylated enzymes faithfully colocalizing with pα-syn*. Pα-syn* directly interacts with tau, which gets phosphorylated by pJNK and pp38 (Fig. 11A). Pα-syn* and ptau aggregate into larger inclusions surrounding the endings of mitochondrial tubules. Concomitantly, GSK3β, which also directly interacts with pα-syn*, contributes to further tau phosphorylation. Pα-syn*/ptau aggregates are toxic, leading to mitochondrial dysfunction and fragmentation (Fig. 11B). Fragmented mitochondria surrounded by pα-syn*/ptau aggregates is tagged for mitophagic degradation by parkin (Fig. 11C). Mitophagic vacuoles are released, containing pα-syn*/ptau, MAPKs, parkin and mitochondrial debris (Fig. 11D).

While it was known that JNK and p38 are biochemically able to phosphorylate tau, we demonstrate that these kinases phosphorylate tau in a pα-syn* dependent way, adding to the previous list of PKA, GSK3β (Duka et al., 2009) and LRRK2 (Kawakami and Ichikawa, 2015) known to be involved in α-synuclein-dependent tau phosphorylation (Kawakami and Ichikawa, 2015; Tenreiro et al., 2014).

MAPKs have been previously implicated in PD pathogenesis, and so has the coexistence of α-syn and tau pathology. Here, we were able to directly link MAPK activation and pα-syn*/ptau aggregates with mitochondrial damage and mitophagy. We propose that pα-syn* acts as the master trigger of both kinase activation and the formation of mitochondrial ptau aggregates, emphasizing the central role of pα-syn* in the pathogenesis of Parkinson's disease and other synucleinopathies.

## Acknowledgments

We thank Prof. Phil LoGrasso for providing us with the brain sections from the BBDP. We are grateful to Shannon Howard for her technical help with mice experiments. Funds to support this work were provided by The Sandy Hill Foundation and by a generous gift from Dr. David P. Brown.

## References

Alonso, A.D., Di Clerico, J., Li, B., Corbo, C.P., Alaniz, M.E., Grundke-Iqbal, I., Iqbal, K., 2010. Phosphorylation of tau at Thr212, Thr231, and Ser262 combined causes neurodegeneration. J. Biol. Chem. 285, 30851–30860.

Arima, K., Ueda, K., Sunohara, N., Arakawa, K., Hirai, S., Nakamura, M., Tonozuka-Uehara, H., Kawai, M., 1998. NACP/alpha-synuclein immunoreactivity in fibrillary components of neuronal and oligodendroglial cytoplasmic inclusions in the pontine nuclei in multiple system atrophy. Acta Neuropathol. 96, 439–444.

Athanassiadou, A., Voutsinas, G., Psiouri, L., Leroy, E., Polymeropoulos, M.H., Ilias, A., Maniatis, G.M., Papapetropoulos, T., 1999. Genetic analysis of families with Parkinson disease that carry the Ala53Thr mutation in the gene encoding alpha-synuclein. Am. J. Hum. Genet. 65, 555–558.

Betarbet, R., Canet-Aviles, R.M., Sherer, T.B., Mastroberardino, P.G., McLendon, C., Kim, J.H., Lund, S., Na, H.M., Taylor, G., Bence, N.F., Kopito, R., Seo, B.B., Yagi, T., Yagi, A., Klinefelter, G., Cookson, M.R., Greenamyre, J.T., 2006. Intersecting pathways to neurodegeneration in Parkinson's disease: effects of the pesticide rotenone on DJ-1, alpha-synuclein, and the ubiquitin-proteasome system. Neurobiol. Dis. 22, 404–420.

Bolte, S., Cordelieres, F.P., 2006. A guided tour into subcellular colocalization analysis in light microscopy. J. Microsc. 224, 213–232.

Chambers, J.W., Pachori, A., Howard, S., Ganno, M., Hansen Jr., D., Kamenecka, T., Song, X., Duckett, D., Chen, W., Ling, Y.Y., Cherry, L., Cameron, M.D., Lin, L., Ruiz, C.H., Lograsso, P., 2011. Small molecule c-Jun-N-terminal kinase (JNK) inhibitors protect dopaminergic neurons in a model of Parkinson's disease. ACS Chem. Neurosci. 2, 198–206.

Chang, L., Jones, Y., Ellisman, M.H., Goldstein, L.S., Karin, M., 2003. JNK1 is required for maintenance of neuronal microtubules and controls phosphorylation of microtubule-associated proteins. Dev. Cell 4, 521–533.

Chang, D., Nalls, M.A., Hallgrimsdottir, I.B., Hunkapiller, J., van der Brug, M., Cai, F., International Parkinson's Disease Genomics, 23andMe Research, Kerchner, G.A., Ayalon, G., Bingol, B., Sheng, M., Hinds, D., Behrens, T.W., Singleton, A.B., Bhangale, T.R., Graham, R.R., 2017. A meta-analysis of genome-wide association studies identifies 17 new Parkinson's disease risk loci. Nat. Genet. 49, 1511–1516.

Charni, S., de Bettignies, G., Rathore, M.G., Aguilo, J.I., van den Elsen, P.J., Haouzi, D., Hipskind, R.A., Enriquez, J.A., Sanchez-Beato, M., Pardo, J., Anel, A., Villalba, M., 2010. Oxidative phosphorylation induces de novo expression of the MHC class I in tumor cells through the ERK5 pathway. J. Immunol. 185, 3498–3503.

Chen, J., Ren, Y., Gui, C., Zhao, M., Wu, X., Mao, K., Li, W., Zou, F., 2018. Phosphorylation of Parkin at serine 131 by p38 MAPK promotes mitochondrial dysfunction and neuronal death in mutant A53T alpha-synuclein model of Parkinson's disease. Cell Death Dis. 9, 700.

Cho, J.H., Johnson, G.V., 2004. Primed phosphorylation of tau at Thr231 by glycogen synthase kinase 3beta (GSK3beta) plays a critical role in regulating tau's ability to bind and stabilize microtubules. J. Neurochem. 88, 349–358.

Choi, W.S., Abel, G., Klintworth, H., Flavell, R.A., Xia, Z., 2010. JNK3 mediates paraquat- and rotenone-induced dopaminergic neuron death. J. Neuropathol. Exp. Neurol. 69, 511–520.

Crittenden, P.L., Filipov, N.M., 2011. Manganese modulation of MAPK pathways: effects on upstream mitogen activated protein kinase kinases and mitogen activated kinase phosphatase-1 in microglial cells. J. Appl. Toxicol. 31, 1–10.

Cuenda, A., 2000. Mitogen-activated protein kinase kinase 4 (MKK4). Int. J. Biochem. Cell Biol. 32, 581–587.

Dawson, T.M., Dawson, V.L., 2003. Rare genetic mutations shed light on the pathogenesis of Parkinson disease. J. Clin. Invest. 111, 145–151.

Di Maio, R., Barrett, P.J., Hoffman, E.K., Barrett, C.W., Zharikov, A., Borah, A., Hu, X., McCoy, J., Chu, C.T., Burton, E.A., Hastings, T.G., Greenamyre, J.T., 2016. Alpha-Synuclein binds to TOM20 and inhibits mitochondrial protein import in Parkinson's disease. Sci. Transl. Med. 8, 342ra378.

Duka, T., Duka, V., Joyce, J.N., Sidhu, A., 2009. Alpha-Synuclein contributes to GSK-3beta-catalyzed Tau phosphorylation in Parkinson's disease models. FASEB J. 23, 2820–2830.

Duka, V., Lee, J.H., Credle, J., Wills, J., Oaks, A., Smolinsky, C., Shah, K., Mash, D.C., Masliah, E., Sidhu, A., 2013. Identification of the sites of tau hyperphosphorylation and activation of tau kinases in synucleinopathies and Alzheimer's diseases. PLoS One 8, e75025.

Dunn, K.W., Kamocka, M.M., McDonald, J.H., 2011. A practical guide to evaluating colocalization in biological microscopy. Am. J. Physiol. Cell Physiol. 300, C723–C742.

Eriksen, J.L., Przedborski, S., Petrucelli, L., 2005. Gene dosage and pathogenesis of Parkinson's disease. Trends Mol. Med. 11, 91–96.

Farrer, M.J., 2006. Genetics of Parkinson disease: paradigm shifts and future prospects. Nat. Rev. Genet. 7, 306–318.

Ferrer, I., Blanco, R., Carmona, M., Puig, B., Barrachina, M., Gomez, C., Ambrosio, S., 2001. Active, phosphorylation-dependent mitogen-activated protein kinase (MAPK/ERK), stress-activated protein kinase/c-Jun N-terminal kinase (SAPK/JNK), and p38 kinase expression in Parkinson's disease and Dementia with Lewy bodies. J. Neural Transm. (Vienna) 108, 1383–1396.

Forman, M.S., Lee, V.M., Trojanowski, J.Q., 2005. Nosology of Parkinson's disease: looking for the way out of a quagmire. Neuron 47, 479–482.

Fox, S.H., Katzenschlager, R., Lim, S.Y., Barton, B., de Bie, R.M.A., Seppi, K., Coelho, M., Sampaio, C., Movement Disorder Society Evidence-Based Medicine Committee, 2018. International Parkinson and movement disorder society evidence-based medicine review: Update on treatments for the motor symptoms of Parkinson's disease. Mov. Disord 33, 1248–1266.

Galvin, J.E., Lee, V.M., Trojanowski, J.Q., 2001. Synucleinopathies: clinical and pathological implications. Arch. Neurol. 58, 186–190.

Gerson, J.E., Farmer, K.M., Henson, N., Castillo-Carranza, D.L., Carretero Murillo, M., Sengupta, U., Barrett, A., Kayed, R., 2018. Tau oligomers mediate alpha-synuclein toxicity and can be targeted by immunotherapy. Mol. Neurodegener. 13, 13.

Grassi, D., Howard, S., Zhou, M., Diaz-Perez, N., Urban, N.T., Guerrero-Given, D., Kamasawa, N., Volpicelli-Daley, L.A., Lograsso, P., Lasmézas, C.I., 2018. Identification of a highly neurotoxic alpha-synuclein species inducing mitochondrial damage and mitophagy in Parkinson's disease. Proc. Natl. Acad. Sci. U. S. A. 115, E2634–E2643.

Guo, J.L., Covell, D.J., Daniels, J.P., Iba, M., Stieber, A., Zhang, B., Riddle, D.M., Kwong, L.K., Xu, Y., Trojanowski, J.Q., Lee, V.M., 2013. Distinct alpha-synuclein strains differentially promote tau inclusions in neurons. Cell 154, 103–117.

Haggerty, T., Credle, J., Rodriguez, O., Wills, J., Oaks, A.W., Masliah, E., Sidhu, A., 2011. Hyperphosphorylated Tau in an alpha-synuclein-overexpressing transgenic model of Parkinson's disease. Eur. J. Neurosci. 33, 1598–1610.

Hansen, C., Angot, E., Bergstrom, A.L., Steiner, J.A., Pieri, L., Paul, G., Outeiro, T.F., Melki, R., Kallunki, P., Fog, K., Li, J.Y., Brundin, P., 2011. Alpha-synuclein propagates from mouse brain to grafted dopaminergic neurons and seeds aggregation in cultured human cells. J. Clin. Invest. 121, 715–725.

Hunot, S., Vila, M., Teismann, P., Davis, R.J., Hirsch, E.C., Przedborski, S., Rakic, P.,

Flavell, R.A., 2004. JNK-mediated induction of cyclooxygenase 2 is required for neurodegeneration in a mouse model of Parkinson's disease. Proc. Natl. Acad. Sci. U. S. A. 101, 665–670.
Irwin, D.J., Lee, V.M., Trojanowski, J.Q., 2013. Parkinson's disease dementia: convergence of alpha-synuclein, tau and amyloid-beta pathologies. Nat. Rev. Neurosci. 14, 626–636.
Kawakami, F., Ichikawa, T., 2015. The role of alpha-Synuclein and LRRK2 in tau phosphorylation. Parkinsons Dis. 2015, 734746.
Ki, C.S., Stavrou, E.F., Davanos, N., Lee, W.Y., Chung, E.J., Kim, J.Y., Athanassiadou, A., 2007. The Ala53Thr mutation in the alpha-synuclein gene in a Korean family with Parkinson disease. Clin. Genet. 71, 471–473.
Kim, E.K., Choi, E.J., 2010. Pathological roles of MAPK signaling pathways in human diseases. Biochim. Biophys. Acta 1802, 396–405.
Klein, C., Schlossmacher, M.G., 2007. Parkinson disease, 10 years after its genetic revolution: multiple clues to a complex disorder. Neurology 69, 2093–2104.
Kordower, J.H., Chu, Y., Hauser, R.A., Freeman, T.B., Olanow, C.W., 2008. Lewy body-like pathology in long-term embryonic nigral transplants in Parkinson's disease. Nat. Med. 14, 504–506.
Kruger, R., Kuhn, W., Muller, T., Woitalla, D., Graeber, M., Kosel, S., Przuntek, H., Epplen, J.T., Schols, L., Riess, O., 1998. Ala30Pro mutation in the gene encoding alpha-synuclein in Parkinson's disease. Nat. Genet. 18, 106–108.
La Vitola, P., Balducci, C., Cerovic, M., Santamaria, G., Brandi, E., Grandi, F., Caldinelli, L., Colombo, L., Morgese, M.G., Trabace, L., Pollegioni, L., Albani, D., Forloni, G., 2018. Alpha-synuclein oligomers impair memory through glial cell activation and via Toll-like receptor 2. Brain Behav. Immun. 69, 591–602.
Lang, A.E., Lozano, A.M., 1998a. Parkinson's disease. First of two parts. N. Engl. J. Med. 339, 1044–1053.
Lang, A.E., Lozano, A.M., 1998b. Parkinson's disease. Second of two parts. N. Engl. J. Med. 339, 1130–1143.
Lasagna-Reeves, C.A., Castillo-Carranza, D.L., Sengupta, U., Clos, A.L., Jackson, G.R., Kayed, R., 2011. Tau oligomers impair memory and induce synaptic and mitochondrial dysfunction in wild-type mice. Mol. Neurodegener. 6, 39.
Li, J.Y., Englund, E., Holton, J.L., Soulet, D., Hagell, P., Lees, A.J., Lashley, T., Quinn, N.P., Rehncrona, S., Bjorklund, A., Widner, H., Revesz, T., Lindvall, O., Brundin, P., 2008. Lewy bodies in grafted neurons in subjects with Parkinson's disease suggest host-to-graft disease propagation. Nat. Med. 14, 501–503.
Lippa, C.F., Schmidt, M.L., Lee, V.M., Trojanowski, J.Q., 1999. Antibodies to alpha-synuclein detect Lewy bodies in many Down's syndrome brains with Alzheimer's disease. Ann. Neurol. 45, 353–357.
Liu, H., Zhou, M., 2017. Antitumor effect of Quercetin on Y79 retinoblastoma cells via activation of JNK and p38 MAPK pathways. BMC Complement. Altern. Med. 17, 531.
Liu, W., Ruiz-Velasco, A., Wang, S., Khan, S., Zi, M., Jungmann, A., Dolores Camacho-Munoz, M., Guo, J., Du, G., Xie, L., Oceandy, D., Nicolaou, A., Galli, G., Muller, O.J., Cartwright, E.J., Ji, Y., Wang, X., 2017. Metabolic stress-induced cardiomyopathy is caused by mitochondrial dysfunction due to attenuated Erk5 signaling. Nat. Commun. 8, 494.
Luk, K.C., Song, C., O'Brien, P., Stieber, A., Branch, J.R., Brunden, K.R., Trojanowski, J.Q., Lee, V.M., 2009. Exogenous alpha-synuclein fibrils seed the formation of Lewy body-like intracellular inclusions in cultured cells. Proc. Natl. Acad. Sci. U. S. A. 106, 20051–20056.
Luk, K.C., Kehm, V., Carroll, J., Zhang, B., O'Brien, P., Trojanowski, J.Q., Lee, V.M., 2012. Pathological alpha-synuclein transmission initiates Parkinson-like neurodegeneration in nontransgenic mice. Science 338, 949–953.
Luth, E.S., Stavrovskaya, I.G., Bartels, T., Kristal, B.S., Selkoe, D.J., 2014. Soluble, prefibrillar alpha-synuclein oligomers promote complex I-dependent, Ca2+ −induced mitochondrial dysfunction. J. Biol. Chem. 289, 21490–21507.
Manczak, M., Reddy, P.H., 2012. Abnormal interaction between the mitochondrial fission protein Drp1 and hyperphosphorylated tau in Alzheimer's disease neurons: implications for mitochondrial dysfunction and neuronal damage. Hum. Mol. Genet. 21, 2538–2547.
Markopoulou, K., Wszolek, Z.K., Pfeiffer, R.F., Chase, B.A., 1999. Reduced expression of the G209A alpha-synuclein allele in familial Parkinsonism. Ann. Neurol. 46, 374–381.
Martin, I., Dawson, V.L., Dawson, T.M., 2011. Recent advances in the genetics of Parkinson's disease. Annu. Rev. Genomics Hum. Genet. 12, 301–325.
Martin, L., Latypova, X., Wilson, C.M., Magnaudeix, A., Perrin, M.L., Yardin, C., Terro, F., 2013. Tau protein kinases: involvement in Alzheimer's disease. Ageing Res. Rev. 12, 289–309.
Olanow, C.W., Tatton, W.G., 1999. Etiology and pathogenesis of Parkinson's disease. Annu. Rev. Neurosci. 22, 123–144.
Pan, J., Li, H., Zhang, B., Xiong, R., Zhang, Y., Kang, W.Y., Chen, W., Zhao, Z.B., Chen, S.D., 2015. Small peptide inhibitor of JNK3 protects dopaminergic neurons from MPTP induced injury via inhibiting the ASK1-JNK3 signaling pathway. PLoS One 10, e0119204.
Pankratz, N., Wilk, J.B., Latourelle, J.C., Destefano, A.L., Halter, C., Pugh, E.W., Doheny, K.F., Gusella, J.F., Nichols, W.C., Foroud, T., Myers, R.H., 2009. Genomewide association study for susceptibility genes contributing to familial Parkinson disease. Hum. Genet. 124, 593–605.
Pickrell, A.M., Youle, R.J., 2015. The roles of PINK1, parkin, and mitochondrial fidelity in Parkinson's disease. Neuron 85, 257–273.
Ray, A., Sehgal, N., Karunakaran, S., Rangarajan, G., Ravindranath, V., 2015. MPTP activates ASK1-p38 MAPK signaling pathway through TNF-dependent Trx1 oxidation in parkinsonism mouse model. Free Radic. Biol. Med. 87, 312–325.
Schapira, A.H., Olanow, C.W., Greenamyre, J.T., Bezard, E., 2014. Slowing of neurodegeneration in Parkinson's disease and Huntington's disease: future therapeutic perspectives. Lancet 384, 545–555.
Sengupta, U., Guerrero-Munoz, M.J., Castillo-Carranza, D.L., Lasagna-Reeves, C.A., Gerson, J.E., Paulucci-Holthauzen, A.A., Krishnamurthy, S., Farhed, M., Jackson, G.R., Kayed, R., 2015. Pathological interface between oligomeric alpha-Synuclein and Tau in synucleinopathies. Biol. Psychiatry 78, 672–683.
Spillantini, M.G., Schmidt, M.L., Lee, V.M., Trojanowski, J.Q., Jakes, R., Goedert, M., 1997. Alpha-synuclein in Lewy bodies. Nature 388, 839–840.
Spillantini, M.G., Crowther, R.A., Jakes, R., Hasegawa, M., Goedert, M., 1998. alpha-Synuclein in filamentous inclusions of Lewy bodies from Parkinson's disease and dementia with lewy bodies. Proc. Natl. Acad. Sci. U. S. A. 95, 6469–6473.
Spira, P.J., Sharpe, D.M., Halliday, G., Cavanagh, J., Nicholson, G.A., 2001. Clinical and pathological features of a Parkinsonian syndrome in a family with an Ala53Thr alpha-synuclein mutation. Ann. Neurol. 49, 313–319.
Su, C., Sun, F., Cunningham, R.L., Rybalchenko, N., Singh, M., 2014. ERK5/KLF4 signaling as a common mediator of the neuroprotective effects of both nerve growth factor and hydrogen peroxide preconditioning. Age (Dordr.) 36, 9685.
Sutherland, C., 2011. What are the bona fide GSK3 Substrates? Int. J. Alzheimers Dis. 2011, 505607.
Tenreiro, S., Eckermann, K., Outeiro, T.F., 2014. Protein phosphorylation in neurodegeneration: friend or foe? Front. Mol. Neurosci. 7, 42.
Volpicelli-Daley, L.A., Luk, K.C., Patel, T.P., Tanik, S.A., Riddle, D.M., Stieber, A., Meaney, D.F., Trojanowski, J.Q., Lee, V.M., 2011. Exogenous alpha-synuclein fibrils induce Lewy body pathology leading to synaptic dysfunction and neuron death. Neuron 72, 57–71.
Volpicelli-Daley, L.A., Gamble, K.L., Schultheiss, C.E., Riddle, D.M., West, A.B., Lee, V.M., 2014a. Formation of alpha-synuclein Lewy neurite-like aggregates in axons impedes the transport of distinct endosomes. Mol. Biol. Cell 25, 4010–4023.
Volpicelli-Daley, L.A., Luk, K.C., Lee, V.M., 2014b. Addition of exogenous alpha-synuclein preformed fibrils to primary neuronal cultures to seed recruitment of endogenous alpha-synuclein to Lewy body and Lewy neurite-like aggregates. Nat. Protoc. 9, 2135–2146.
Wang, W., Shi, L., Xie, Y., Ma, C., Li, W., Su, X., Huang, S., Chen, R., Zhu, Z., Mao, Z., Han, Y., Li, M., 2004. SP600125, a new JNK inhibitor, protects dopaminergic neurons in the MPTP model of Parkinson's disease. Neurosci. Res. 48, 195–202.
Wu, R., Chen, H., Ma, J., He, Q., Huang, Q., Liu, Q., Li, M., Yuan, Z., 2016. C-Abl-p38alpha signaling plays an important role in MPTP-induced neuronal death. Cell Death Differ. 23, 542–552.
Xia, X.G., Harding, T., Weller, M., Bieneman, A., Uney, J.B., Schulz, J.B., 2001. Gene transfer of the JNK interacting protein-1 protects dopaminergic neurons in the MPTP model of Parkinson's disease. Proc. Natl. Acad. Sci. U. S. A. 98, 10433–10438.
Yamasaki, T., Kawasaki, H., Nishina, H., 2012. Diverse Roles of JNK and MKK Pathways in the Brain. J. Signal. Transduct. 2012, 459265.
Yoon, S.O., Park, D.J., Ryu, J.C., Ozer, H.G., Tep, C., Shin, Y.J., Lim, T.H., Pastorino, L., Kunwar, A.J., Walton, J.C., Nagahara, A.H., Lu, K.P., Nelson, R.J., Tuszynski, M.H., Huang, K., 2012. JNK3 perpetuates metabolic stress induced by Abeta peptides. Neuron 75, 824–837.
Yun, S.P., Kim, D., Kim, S., Kim, S., Karuppagounder, S.S., Kwon, S.H., Lee, S., Kam, T.I., Lee, S., Ham, S., Park, J.H., Dawson, V.L., Dawson, T.M., Lee, Y., Ko, H.S., 2018. Alpha-Synuclein accumulation and GBA deficiency due to L444P GBA mutation contributes to MPTP-induced parkinsonism. Mol. Neurodegener. 13, 1.
Zarranz, J.J., Alegre, J., Gomez-Esteban, J.C., Lezcano, E., Ros, R., Ampuero, I., Vidal, L., Hoenicka, J., Rodriguez, O., Atares, B., Llorens, V., Gomez Tortosa, E., del Ser, T., Munoz, D.G., de Yebenes, J.G., 2004. The new mutation, E46K, of alpha-synuclein causes Parkinson and Lewy body dementia. Ann. Neurol. 55, 164–173.
Zhao, F., Bi, L., Wang, W., Wu, X., Li, Y., Gong, F., Lu, S., Feng, F., Qian, Z., Hu, C., Wu, Y., Sun, Y., 2016. Mutations of glucocerebrosidase gene and susceptibility to Parkinson's disease: an updated meta-analysis in a European population. Neuroscience 320, 239–246.
Zinchuk, V., Grossenbacher-Zinchuk, O., 2014. Quantitative colocalization analysis of fluorescence microscopy images. Curr. Protoc. Cell Biol. 4 (19), 11–14 62:Unit.